Journal of Biomechanics 83 (2019) 165–173

Contents lists available at ScienceDirect

Journal of Biomechanics

journal homepage: www.elsevier.com/locate/jbiomech
www.JBiomech.com

# Evaluation of a method to scale muscle strength for gait simulations of children with cerebral palsy

Amy K. Hegarty [a], Trey V. Hulbert [a], Max J. Kurz [b], Wayne Stuberg [b], Anne K. Silverman [a,*]

[a] Department of Mechanical Engineering, Colorado School of Mines, Golden, CO 80401, United States
[b] Department of Physical Therapy, Munroe-Meyer Institute for Genetics and Rehabilitation, University of Nebraska Medical Center, Omaha, NE 68198, United States

ARTICLE INFO

*Article history:*
Accepted 23 November 2018

*Keywords:*
Musculoskeletal modeling
Biomechanics
Pathological gait
Muscle strength
Strength scaling

ABSTRACT

Cerebral palsy (CP) is a neurological disorder that results in life-long mobility impairments. Musculoskeletal models used to investigate mobility deficits for children with CP often lack subject-specific characteristics such as altered muscle strength, despite a high prevalence of muscle weakness in this population. We hypothesized that incorporating subject-specific strength scaling within musculoskeletal models of children with CP would improve accuracy of muscle excitation predictions in walking simulations. Ten children (13.5 ± 3.3 years; GMFCS level II) with spastic CP participated in a gait analysis session where lower-limb kinematics, ground reaction forces, and bilateral electromyography (EMG) of five lower-limb muscles were collected. Isometric strength was measured for each child using handheld dynamometry. Three musculoskeletal models were generated for each child including a 'Default' model with the generic musculoskeletal model's muscle strength, a 'Uniform' model with muscle strength scaled allometrically, and a 'Custom' model with muscle strength scaled based on handheld dynamometry strength measures. Muscle-driven gait simulations were generated using each model for each child. Simulation accuracy was evaluated by comparing predicted muscle excitations and measured EMG signals, both in the duration of muscle activity and the root-mean-square difference (RMSD) between signals. Improved agreement with EMG were found in both the 'Custom' and 'Uniform' models compared to the 'Default' model indicated by improvement in RMSD summed across all muscles, as well as RMSD and duration of activity for individual muscles. Incorporating strength scaling into musculoskeletal models can improve the accuracy of walking simulations for children with CP.



## 1. Introduction

Children with cerebral palsy (CP) often have reduced muscle strength and volume compared to their typically developing peers (Dallmeijer et al., 2017; Eek et al., 2011; Elder et al., 2003; Oberhofer et al., 2010). These strength deficits are often associated with altered posture and movement strategies, and are compounded by common treatments for underlying spasticity, contracture and short muscle-tendon units (Zhou et al., 2017). Changes in lower-limb muscle volume are also highly variable between muscle groups and across children with CP (Handsfield et al., 2016).

Musculoskeletal simulations have been used to investigate neuromuscular function in able-bodied individuals (e.g., Liu et al., 2006; Neptune et al., 2001), as well as those with CP (e.g., Fox et al., 2009; Hegarty et al., 2016; Steele et al., 2013). However, developing musculoskeletal models that are representative of CP is challenging, and thus clinical translation of these models can also be limited. Generic musculoskeletal models, based on detailed cadaveric studies of a small set of healthy adults (e.g., Friederich and Brand, 1990; Klein Horsman et al., 2007; Wickiewicz et al., 1983), are typically scaled and applied for studies measuring able-bodied and pathological populations without consideration of altered musculotendon properties. Closing the gap between generic and subject-specific musculoskeletal models has the potential for improving simulation accuracy and clinical translation.

Previous studies have shown the importance of incorporating subject-specific musculotendon parameters on the accuracy of musculoskeletal simulation predictions of joint contact forces (Serrancolí et al., 2016) and muscle activation patterns (Knarr et al., 2014). Subject-specific estimates of maximum isometric force, optimal fiber length, or tendon slack length incorporated into musculoskeletal models using magnetic resonance imaging have improved simulation quality (Bolsterlee et al., 2015; Modenese et al., 2018). However, obtaining image-based estimates of

* Corresponding author at: Department of Mechanical Engineering, Colorado School of Mines, 1500 Illinois Street, Golden, CO 80401, United States.
*E-mail address:* asilverm@mines.edu (A.K. Silverman).

https://doi.org/10.1016/j.jbiomech.2018.11.037
0021-9290/

subject-specific muscle properties is not always feasible. Previous work has proposed various approaches for scaling muscle strength in healthy populations, such as scale factors derived from body size and height (e.g., Folland et al., 2008; Handsfield et al., 2014), body mass (e.g., Van der Krogt et al., 2016), and estimated muscle mass based on anthropometry (e.g., Correa and Pandy, 2011). Subject-specific estimates of maximum isometric muscle force have also been quantified using strength assessments such as isometric dynamometry or burst superposition, improving simulation accuracy for individuals with instrumented implants and individuals post-stroke (Knarr et al., 2014; Knarr and Higginson, 2015).

Muscle strength scaling clearly has the capacity to improve the accuracy of musculoskeletal simulation for both healthy and impaired populations. As individuals with CP often incur widespread and variable muscle weakness, effective and practical subject-specific scaling techniques that improve the accuracy of musculoskeletal simulations are important to develop. The purpose of this study was to evaluate the effects of (1) allometric strength scaling, consistent with typically developing child strength, and (2) joint level strength scaling, based on clinically measured joint strength, on the accuracy of predicted muscle excitations in gait simulations of children with CP. We hypothesized that joint level, measurement-driven strength scaling would improve the agreement of simulated muscle excitations with measured electromyography (EMG) in all measured lower-limb muscles compared to typically developing strength scaling and to no strength scaling. This work expands on previous literature evaluating subject-specific scaling for children with CP (e.g., Correa et al., 2011) by evaluating a subject-specific scaling approach using handheld dynamometry measures of joint strength through walking simulation agreement with electromyography.

## 2. Methods

### 2.1. Experimental data collection

Ten children with spastic CP (6 diplegic, 4 hemipelegic, age: 13.5 ± 3.3 yrs., mass: 46.4 ± 16.3 kg, height: 1.52 ± 0.17 m, Gross Motor Function Classification System level II) participated in the experimental protocol approved by the University's Committee for the Protection of Human Subjects. All participants' legal guardians provided written consent and all children gave their assent to participate. All children walked barefoot and independently with no assistive devices during the gait analysis session. No child had undergone tendon transfer surgeries or undergone surgery or botulinum toxin-A injections within the six months prior to participating. One physical therapist (WS), board certified in pediatrics and with over 40 years of clinical experience, completed the musculoskeletal exams of the participants. Standardized protocols were used for both musculoskeletal exam procedures and handheld dynamometry (Malanga and Mautner, 2017). Children with fixed contractures or a modified Ashworth score of three or greater of the ankle, knee of hip musculature were excluded from the study (Pandyan et al., 1999). Tibial torsion was recorded with a goniometer and standardized protocol (Stuberg et al., 1991) and patella alta was determined via palpation. Participants with variation from normative values of greater than 30 degrees of tibiofibular torsion or patella alta, Insall-Salvate ratio > 1, were excluded from the study. Normative values and also reliability of similarly recorded musculoskeletal measures are reported by Mudge et al. (2014).

Isometric strength was tested for hip flexion/extension, hip abduction, knee flexion/extension, and ankle plantarflexion/dorsiflexion. Tests were performed bilaterally in neutral gravity positions (Kurz et al., 2011; Table 1) and the children exerted their maximum force against static resistance while output force was measured by a handheld dynamometer (Hoggan Health Industries, West Jordan, UT), which provides reliable measures of lower extremity muscular strength in children with CP (Crompton et al., 2007). Dynamometry scores were recorded using a "make test" procedure as the licensed physical therapist stabilized the dynamometer and gave verbal encouragement for two, five second isometric contractions. The highest score was recorded. Each child's more affected lower-limb was defined as the limb with the lower total summed strength, measured by handheld dynamometry.

Three-dimensional kinematic marker data were collected during self-selected walking using an eight-camera motion capture system (120 Hz, Vicon Motion Systems, Ltd., Oxford, UK) while ground reaction forces (GRFs) were collected from four force plates (960 Hz, AMTI, Inc., Watertown, MA). Sixteen lower body markers were used to track lower-limb and pelvic kinematics. Corresponding EMG data were collected for five lower-limb muscles bilaterally including the gastrocnemius, medial hamstring, rectus femoris, tibialis anterior, and vastus lateralis (1200 Hz, Delsys, Inc., Natick, MA).

### 2.2. Musculoskeletal models

A generic musculoskeletal model with 14 rigid body segments, 23 degrees of freedom, and 92 musculotendon actuators with force-length-velocity properties (Anderson and Pandy, 2001, 1999; Delp et al., 1990; Yamaguchi and Zajac, 1989; Zajac, 1989) in OpenSim 3.2 (simtk.org) represented each child. Passive torsional actuators were applied to each lower-limb joint to model the effect of passive tissues (Anderson, 1999). The generic musculoskeletal model was scaled in mass and segment size for each participant. The distribution of body mass was preserved through the scaling process, and segment size was scaled based on the distance between segment landmarks measured during a static standing trial. Segment and muscle geometric parameters were scaled based on segment length including segment center of mass, muscle paths, muscle fiber lengths, and tendon slack lengths. Muscle strength, defined by maximum isometric force, was not scaled and was representative of a healthy adult ('Default' model).

### 2.3. Strength scaling

The first model ('Default'), which included scaled body mass, segment size, and musculotendon lengths, was used as the base model for the remaining scaling tasks. The strength of the second model ('Uniform') was scaled to represent typically developing muscle strength. The maximum isometric force value for each lower-limb muscle was scaled by a single uniform scale factor $s_{uniform}$, calculated from the ratio of the child's height ($h_{child}$) and mass ($m_{child}$) to the generic model's height ($h_{generic}$) and mass ($m_{generic}$) (Eq. (1), Handsfield, 2014).

$$s_{uniform} = \frac{h_{child} \times m_{child}}{h_{generic} \times m_{generic}} \quad (1)$$

As many children with CP have non-uniform muscle weakness (Handsfield et al., 2016), joint level strength scaling was also used to generate a third scaled model ('Custom').

Within the 'Custom' model, maximum isometric force values were adjusted by custom scale factors for muscles within each joint group tested with handheld dynamometry. Custom scale values were calculated by replicating the isometric strength tests within a musculoskeletal simulation framework (Fig. 1). The 'Uniform' musculoskeletal model was constrained to the static pose of

**Table 1**
Lower-limb isometric strength tests and the poses used for the 'Custom' model. Muscles within the musculoskeletal model scaled during each simulated strength test are also indicated. Each muscle was included in a clinical strength test scale group if the muscle's moment arm produced a resistive joint torque in the clinical test pose of interest. The muscle that met the maximum excitation criteria during the simulated strength test is indicated (**). Muscle excitations from the gait simulations compared to measured EMG signals during walking are also indicated (E1-E5).

| Clinical isometric strength test | Clinical exam pose | Muscles scaled |
|---|---|---|
| Hip flexion | Supine position<br>Hip, knee, and ankle at 90° flexion bilaterally | Gluteus medius (anterior compartment)<br>Gluteus minimus (anterior compartment)<br>Iliacus<br>Psoas<br>Rectus femoris**, E4<br>Sartorius<br>Tensor fasciae latae |
| Hip extension | Supine position<br>Hip, knee, and ankle at 90° flexion bilaterally | Adductor longus<br>Adductor magnus (anterior, middle, and posterior compartments)<br>Biceps femoris long head<br>Gluteus maximus (superior, middle, and inferior compartments)<br>Gluteus medius (posterior compartment)<br>Gluteus minimus (posterior compartment)<br>Semimembranosus**, E3<br>SemitendinosusE3 |
| Hip abduction | Supine position<br>Hip and knee at 0° flexion, ankle at 90° flexion bilaterally | Gluteus maximus (superior compartment)<br>Gluteus medius (anterior**, middle, and posterior compartments)<br>Gluteus minimus (anterior, middle, and posterior compartments)<br>Pirformis<br>Sartorious<br>Tensor fasciae latae |
| Knee flexion | Sitting position<br>Hip, knee, and ankle at 90° flexion bilaterally | Biceps femoris long head<br>Biceps femoris short head**<br>Gastrocnemius (medial and lateral heads)**, E2<br>Gracilis<br>Sartorious<br>SemimembranosusE3<br>Semitendinosus |
| Knee extension | Sitting position<br>Hip, knee, and ankle at 90° flexion bilaterally | Rectus femorisE4<br>Vastus medialis,<br>Vastus intermedius<br>Vastus lateralis**, E5 |
| Ankle dorsiflexion | Supine position<br>Hip and knee at 0° flexion, ankle at 90° flexion bilaterally | Extensor digitorum longus<br>Extensor hallucis longus<br>Peroneus tertius<br>Tibialis anterior**, E1 |
| Ankle plantarflexion | Supine position<br>Hip and knee at 0° flexion, ankle at 90° flexion bilaterally | Flexor digitorum longus<br>Flexor halluces longus<br>Gastrocnemius (medial and lateral heads)E2<br>Peroneus brevis<br>Peroneus longus<br>Soleus**<br>Tibialis posterior |

each isometric strength test, with all model joints locked except the joint of interest (e.g., for the hip extension test, sagittal plane rotation of the hip was not constrained, Table 1). External forces, measured from the handheld dynamometer, were applied to the musculoskeletal model at the approximate location and orientation of the applied force from the physical therapist during strength testing. Computed Muscle Control (CMC, Thelen et al., 2003) was then used to estimate the muscle forces required to resist motion due to the applied force for each strength test. An iterative scaling approach was implemented within MATLAB to ensure at least one muscle within the joint group was maximally activated (excitation > 0.95) while the model also maintained the static posture (peak RMS joint angle tracking error < 5.5° across all tested strength conditions), without the use of reserve, or non-physiological, actuators (peak torque < 0.1 Nm) at the joint. All muscle maximum isometric forces were initially set to the 'Uniform' model values. After each iteration of the simulated strength test, the excitation of each muscle in the joint group was evaluated against the excitation threshold. When no muscle in the test group exceeded the excitation threshold, the maximum isometric force value for all muscles in the test group were linearly scaled based on the current iteration's excitation signal, and the test was simulated again. The simulated test was repeated until the criteria were met. All muscles crossing the joint of interest with the capacity to generate joint torque in the direction of interest were included in the muscle group to be scaled (Table 1). Scale factors for each joint strength test were generated independently and applied to the 'Custom' scaled model after all joint strength tests were completed. Muscles included in more than one joint strength test were adjusted by the average scale factor for all relevant strength tests. Muscles un-tested by the clinical strength tests were unchanged from the 'Uniform' model.

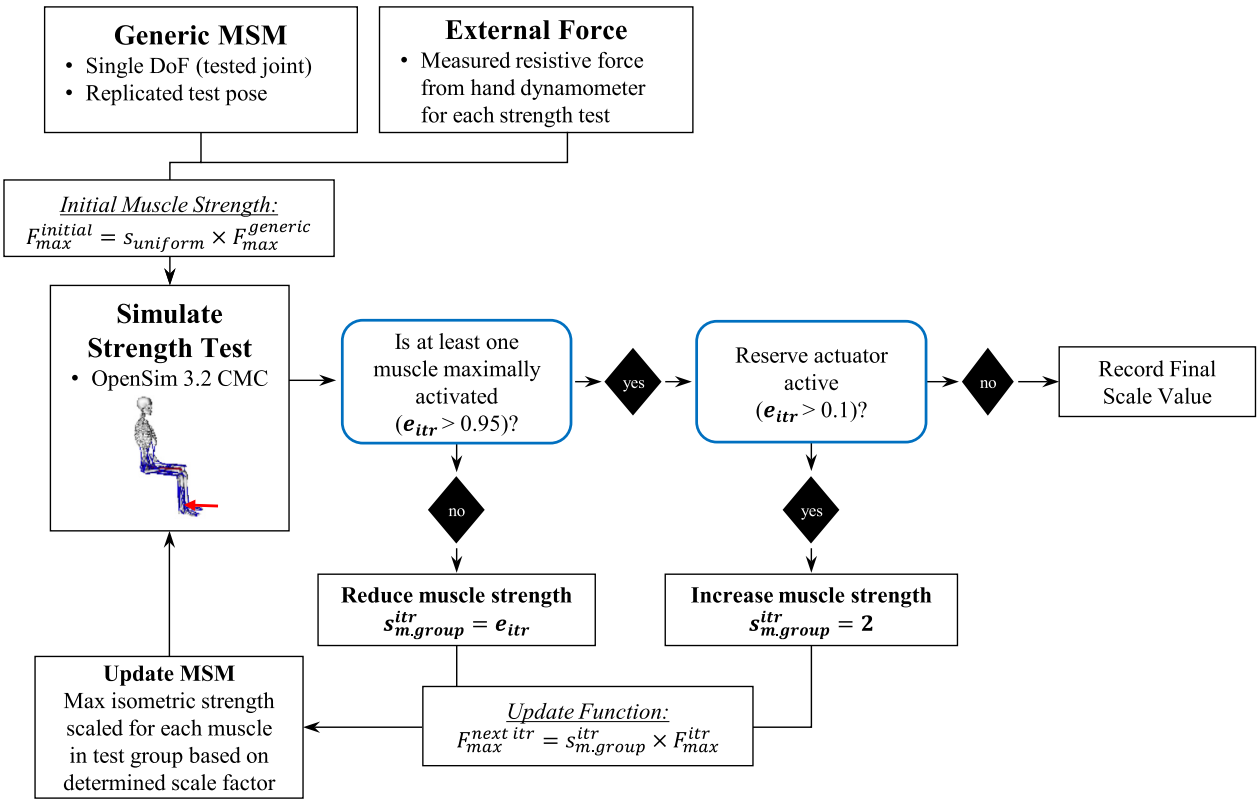


**Fig. 1.** Workflow of the subject-specific strength scaling method used to adjust muscle strength in the 'Custom' model. The generic musculoskeletal model (MSM) is scaled using an iterative approach as shown. The initial maximum isometric force value ($F_{max}^{initial}$) for each muscle is set to the 'Uniform' model values. The clinical strength test is simulated using computed muscle control (CMC). Results of the simulated strength test are evaluated and maximum isometric force estimates ($F_{max}^{nextitr}$) of the tested joint group are updated based on excitation from both the most activated muscle ($e_{itr}$), and the reserved joint actuator ($e_{itr}$). The maximum isometric force values for the joint group muscles are based on calculated scale factors ($s_{m.group}^{nextitr}$). This process was repeated for each joint strength test.

### 2.4. Gait simulations

Gait simulations were developed for three walking trials for each child. Kinematic and GRF data were filtered with a second order low-pass bidirectional Butterworth filter with a cutoff frequency of 6 Hz. An inverse kinematics (IK) model in Visual3D (C-Motion, Inc., Germantown, MD) with the same degrees of freedom as the OpenSim musculoskeletal model, was used within a least-squares optimization to determine the IK solution for each walking trial (Lu and O'Connor, 1999). The IK solution as well as the GRFs for each trial were then input into OpenSim's residual reduction algorithm (RRA, Delp et al., 2007) to improve dynamic consistency and estimate trunk-pelvis kinematics for each walking trial. The three different musculoskeletal models resulting from the different scaling conditions ('Default', 'Uniform' and 'Custom') were then used to generate muscle-driven gait simulations for each walking trial using CMC, resulting in nine simulations for each child.

### 2.5. Data analysis

Musculoskeletal simulation accuracy for the three different scaling conditions was evaluated by comparing the estimated muscle excitations from the gait simulations to measured EMG signals for corresponding muscles (Table 1). EMG signals for each walking trial were band-pass filtered using a second order bidirectional Butterworth filter between 20 Hz and 500 Hz, demeaned, and rectified. Measured EMG signals and simulated excitation signals were both smoothed with a second order low-pass bidirectional Butterworth filter with a cutoff frequency of 2.5 Hz. The amplitude of the smoothed EMG signal was normalized to a peak value of 1 for each gait trial to allow for comparison with the predicted excitation signals from simulation reported between 0 and 1. Each signal was also time normalized to the gait cycle and the root-mean-square (RMS) difference (RMSD) between the processed simulated excitation curve and the processed electromyographic signal was calculated. The RMSD metric reflected changes in both amplitude and timing of the predicted excitations compared to EMG. RMSD between the EMG and simulation signals was computed for each muscle, as well as summed across all muscles for a single model performance metric. RMSD metrics were averaged across the three walking trials for each child. In addition, differences in the timing between the EMG and predicted excitation signals were evaluated by comparing the total duration of muscle activity for each gait cycle. Duration of muscle activity was defined as the total percent of the gait cycle when the EMG or predicted excitation signal exceeded 20% of the peak signal value for that gait trial.

Across the three different scaling conditions, RMSD and difference in duration of muscle activity was compared for each muscle as well as for the total summed difference across all muscles (RMSD only). The RMSD and duration of muscle activity difference for each muscle excitation was compared using a linear mixed effects model, with two fixed effects factors (Scaling Condition × Limb) and a random intercept and slope (Limb) effect generated for each participant, constraining the model to a repeated measures design. Similarly, the total summed RMSD was compared using a repeated measures linear mixed effects model, with one fixed effects factor (Scaling Condition). The influence of each factor within the model was compared using an ANOVA F-test ($\alpha = 0.05$). When significant main effects or interactions were found, post hoc pairwise comparisons with Tukey multiple comparison adjustments were completed ($\alpha = 0.05$).

## 3. Results

Simulation quality was high for all walking simulations with RMS pelvis residual forces and moments of 1.4 ± 0.6% BW, 1.6 ± 0.6% BW-m, and RMS kinematic errors of 1.38 ± 1.30° across all lower-limb joints, and 2.0 ± 1.1 cm averaged across the three translational degrees of freedom in the pelvis. Reserve actuators were also low with RMS joint torques 0.64 ± 0.54% BW-m across all lower-limb joints. RMSD and duration of muscle activity was not assessed for the more affected rectus femoris for participant 06 and bilateral gastrocnemius for participant 04 due to poor EMG signal quality.

### 3.1. Strength scale factors

The 'Custom' strength scaled model had unique strength distributions for each child. The muscle for each muscle group that met the convergence criterion was consistent across all participants for each strength test (Table 1). Five of the participants' lower-limb strength, defined in the 'Custom' model was on average, smaller than the 'Uniform' model, with the largest strength deficits observed at the ankle (Table 2). The 'Uniform' model was also substantially weakened relative to the 'Default' model with an average scaled strength factor of 0.540 ± 0.240. The hip flexors, hip extensors, and knee flexors often resulted in a higher strength in the 'Custom' model compared to the 'Uniform' scaled model, while the knee extensors, ankle plantarflexors, and ankle dorsiflexors were all measured with reduced or equal strength to the 'Uniform' model (Table 2).

### 3.2. Curve comparison – RMSD

Muscle strength scaling had a significant effect ($p = 0.006$) on the agreement of summed RMSD across all muscles between simulated excitation and EMG signals (Fig. 2). Both the 'Custom' (CUST) model and the 'Uniform' model (UNIF) had significantly lower summed RMSD compared to the 'Default' (DEF) model (CUST-DEF $p = 0.007$, UNIF-DEF $p = 0.035$).

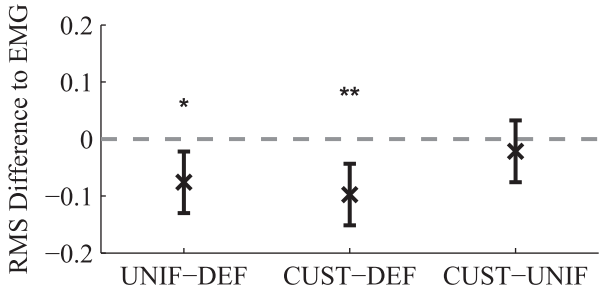


**Fig. 2.** Summed RMSD across all measured lower-limb muscles, compared between simulated excitation signals and measured electromyography (EMG). Pairwise comparisons between the RMSD for each model including 'Default' model (DEF), 'Uniform' model (UNIF) and 'Custom' model (CUST) is shown as an averaged value across participants with Tukey adjusted 95% confidence intervals. Each comparison is shown relative to zero, which would indicate no difference between model generated RMSD. Values lower than zero indicate lower RMS differences to EMG for the first listed model (e.g., the 'Uniform' model had lower RMS differences to EMG compared to the 'Default' model). Significant differences between groups are indicated ('*', $p < 0.05$, '**', $p < 0.01$).

Muscle strength scaling affected RMSD of predicted muscle excitation for individual lower-limb muscles ($p < 0.001$). There were no significant limb or interaction effects for the tested models. Both the 'Custom' and the 'Uniform' models' RMSD to EMG were lower than the 'Default' model for the gastrocnemius (CUST-DEF $p < 0.001$, UNIF-DEF $p = 0.018$), medial hamstrings (CUST-DEF $p = 0.039$, UNIF-DEF $p < 0.001$), and vastus lateralis (CUST-DEF $p < 0.001$, UNIF-DEF $p = 0.009$, Fig. 3) muscles. In addition, the 'Custom' model RMSD was lower than the 'Uniform' model for the vastus lateralis ($p = 0.008$, Fig. 3).

### 3.3. Timing comparison – duration of muscle activity

Muscle strength scaling had a significant effect on the agreement in duration of activity of simulated excitations with EMG

**Table 2**
Strength scaling factors relative to the 'Uniform' model strength for each study participant (P01-P10) as well as the mean (standard deviation) across participants, computed from simulated clinical isometric strength tests. Unmeasured strength tests are indicated (NT) for individuals who were unable to achieve the neutral angle required for the testing pose. Measured strength that exceeded measurement capacity of the handheld dynamometry were considered to have equal strength as the 'Uniform' model (†).

| Participants | | Hip extension | Hip flexion | Hip abduction | Knee extension | Knee flexion | Ankle plantarflexion | Ankle dorsiflexion |
|---|---|---|---|---|---|---|---|---|
| P01 | More affected | 1.000 | 2.000 | 1.000 | 0.435 | 1.000 | 1.000† | 0.456 |
| | Less affected | 1.000 | 2.000 | 1.000 | 0.470 | 1.000 | 1.000† | 0.475 |
| P02 | More affected | 1.000 | 0.811 | 0.936 | 0.791 | 1.000 | 1.000† | 0.656 |
| | Less affected | 1.000 | 1.000 | 1.000 | 1.000 | 1.000 | 1.000† | 0.673 |
| P03 | More affected | 1.000 | 0.857 | 0.640 | 0.456 | 0.696 | 0.268 | 0.934 |
| | Less affected | 1.000 | 0.897 | 0.572 | 0.489 | 0.696 | 0.332 | NT |
| P04 | More affected | 0.744 | 2.000 | 0.940 | 0.547 | 1.000 | 0.504 | 0.636 |
| | Less affected | 1.000 | 2.000 | 1.000 | 0.587 | 2.000 | 0.621 | 0.737 |
| P05 | More affected | 0.779 | 1.000 | 0.711 | 0.396 | 1.000 | 0.157 | NT |
| | Less affected | 0.900 | 1.000 | 0.711 | 0.483 | 1.000 | 0.264 | 0.579 |
| P06 | More affected | 2.000 | 2.000 | 1.000 | 1.000 | 1.772 | 0.400 | 0.534 |
| | Less affected | 2.000 | 2.000 | 1.000 | 1.000 | 1.000 | 0.548 | 1.000 |
| P07 | More affected | 1.000 | 2.000 | 1.000 | 0.649 | 1.000 | 0.171 | NT |
| | Less affected | 2.000 | 3.429 | 1.000 | 1.000 | 1.000 | 0.721 | 0.568 |
| P08 | More affected | 1.000 | 2.000 | 1.000 | 0.756 | 2.000 | 0.308 | NT |
| | Less affected | 1.000 | 2.000 | 1.000 | 0.715 | 2.000 | 0.327 | NT |
| P09 | More affected | 1.000 | 1.000 | 0.601 | 0.462 | 1.000 | NT | NT |
| | Less affected | 1.000 | 1.000 | 0.826 | 0.792 | 1.000 | 0.331 | 0.444 |
| P10 | More affected | 3.999 | 4.542 | 2.597 | 0.705 | 3.277 | NT | NT |
| | Less affected | 4.122 | 4.891 | 2.597 | 0.799 | 3.415 | NT | NT |
| Average | More affected | 1.352 (0.993) | 1.821 (1.099) | 1.043 (0.569) | 0.620 (0.195) | 1.375 (0.780) | 0.301 (0.134) | 0.643 (0.181) |
| | Less affected | 1.502 (1.013) | 2.022 (1.274) | 1.071 (0.558) | 0.733 (0.220) | 1.411 (0.832) | 0.449 (0.178) | 0.639 (0.189) |

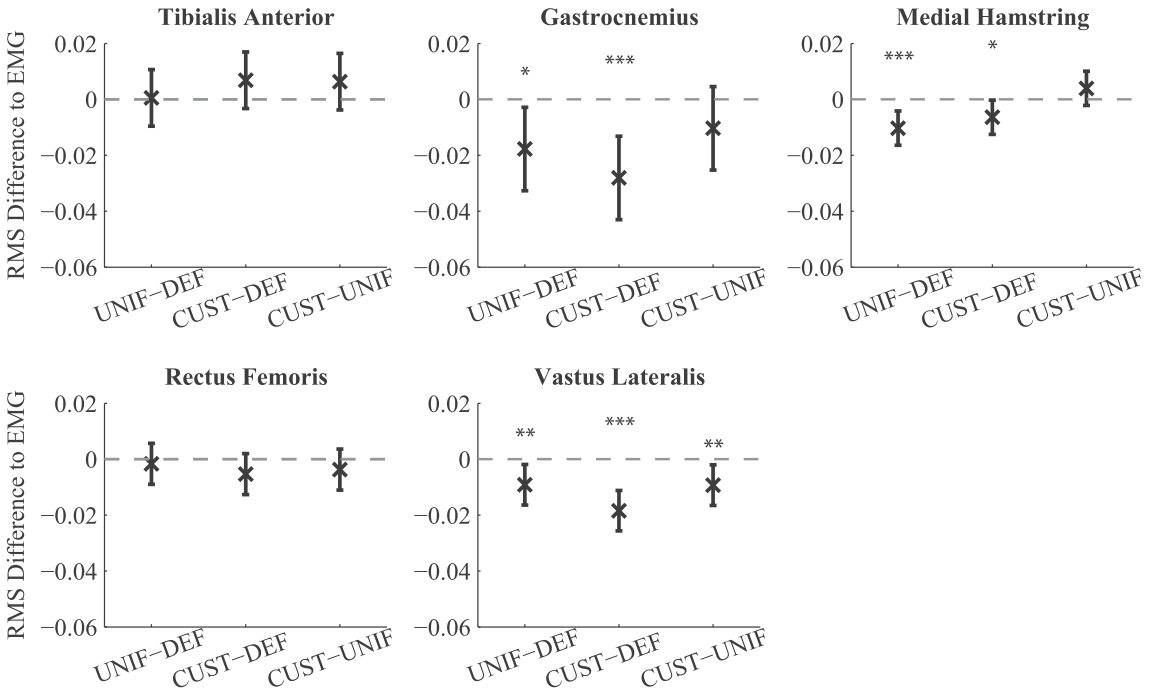


**Fig. 3.** RMSD for each lower-limb muscle, compared between simulated excitation signal and measured electromyography (EMG). Pairwise comparisons between the RMSD for each model including 'Default' model (DEF), 'Uniform' model (UNIF) and 'Custom' model (CUST) is shown as an averaged value across participants with Tukey adjusted 95% confidence intervals. Significant differences between groups are indicated ('*', $p < 0.05$, '**', $p < 0.01$, '***', $p < 0.001$).

**Table 3**
The duration of muscle activity, normalized as a total percent of the gait cycle, is shown for each muscle in the analysis. Duration of activity is reported for the measured EMG signals. Difference in duration of activity from the predicted excitation signals are also shown for the 'Default', 'Uniform', and 'Custom' models. The metrics are reported as the mean +/− standard deviation across all study participants. Significant differences between the 'Default' model response and 'Uniform' or 'Custom' response are shown (†).

| Muscle | EMG duration of activity (% gait cycle) | 'Default' model duration of muscle activity difference to EMG | 'Uniform' model duration of muscle activity difference to EMG | 'Custom' model duration of muscle activity difference to EMG |
|---|---|---|---|---|
| Tibialis anterior | 55.6 ± 14.6 | 8.4 ± 21.1 | 8.5 ± 19.7 | 13.9 ± 18.7 |
| Gastrocnemius | 62.3 ± 12.2 | 18.4 ± 13.8 | 10.0 ± 11.5† | 8.9 ± 13.0† |
| Medial hamstring | 55.6 ± 11.7 | 27.9 ± 14.7 | 26.1 ± 15.0 | 25.6 ± 18.1 |
| Rectus femoris | 65.7 ± 9.9 | 18.1 ± 12.5 | 9.4 ± 14.3† | 5.8 ± 13.2† |
| Vastus lateralis | 59.7 ± 6.35 | 36.2 ± 9.07 | 35.1 ± 10.6 | 33.3 ± 9.8 |

($p < 0.004$). There were no significant limb or interaction effects for the tested models. Both the 'Custom' and 'Uniform' models' duration of muscle activity difference to EMG were lower than the 'Default' model for the gastrocnemius (CUST-DEF $p < 0.007$, UNIF-DEF $p = 0.017$) and rectus femoris (CUST-DEF $p < 0.001$, UNIF-DEF $p = 0.007$, Table 3).

## 4. Discussion

The purpose of this study was to generate and evaluate the use of subject-specific strength scaling on the accuracy of simulated muscle excitations for children with CP. Our hypotheses were partially supported in that we found the 'Custom' model improved overall agreement between EMG and predicted excitation when compared to the 'Default' model. At an individual muscle level, the 'Custom' model improved overall amplitude and timing agreement, quantified by RMSD in the gastrocnemius, medial hamstring, and vastus lateralis. Similarly, the 'Custom' model improved timing agreement quantified by the duration of activity of the gastrocnemius and rectus femoris. However, we were unable to conclude that the 'Custom' model provided better agreement to EMG compared to the 'Uniform' model, except in overall amplitude and timing agreement of the vastus lateralis.

Subject-specific strength scaling did not improve muscle excitation agreement for all subjects in this analysis, or for all lower-limb muscle groups measured in this study. Generally, the strongest improvements in agreement were found for extensor muscles. We suspect that the poor agreement in the ankle dorsiflexors may have stemmed from limited ability to measure active muscle strength in this muscle group using handheld dynamometry. Several children in this analysis (5/10) were unable to complete the dorsiflexion strength assessment, because they were unable to maintain the required gravity neutral joint position. The agreement in duration of muscle activity for the rectus femoris was significantly improved for both the 'Uniform' and 'Custom' scaled models; however, this improvement was not reflected in RMSD. The RMS agreement with EMG for the medial hamstrings was significantly improved for the 'Uniform' and 'Custom' scaled models; however, this improvement was not observed in duration of activity. Thus, scaling of medial hamstrings strength primarily affected the amplitude of the predicted excitation curve without altering timing. As a comparison between the amplitude of the EMG signal and predicted excitation can be adjusted based on the normalization factor used to scale the EMG signal, it is challenging to interpret the significance of results in the medial hamstrings.

Our results suggest that the 'Custom' scaling method has the greatest potential to improve simulation accuracy for muscle

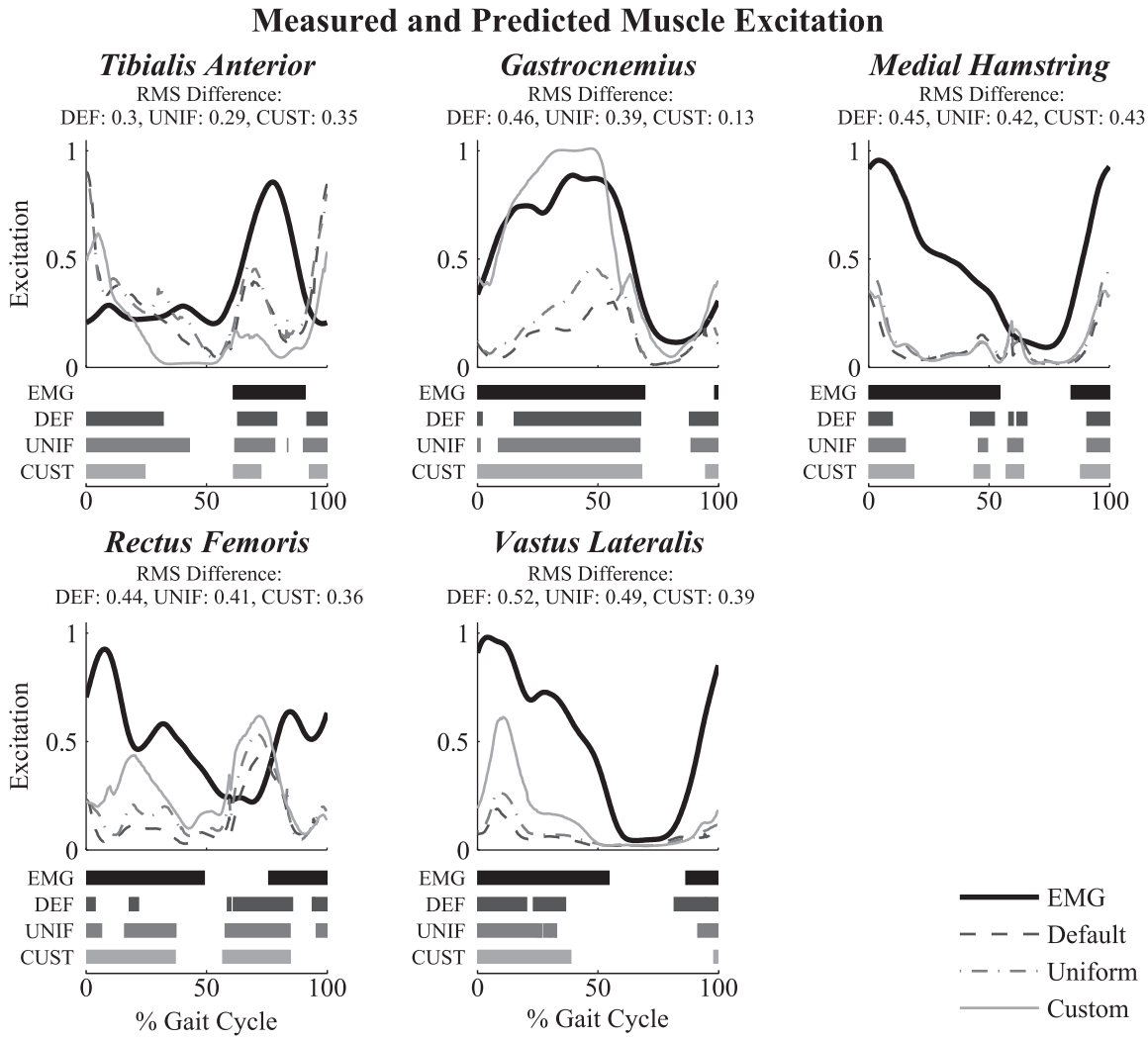


**Fig. 4.** Representative example of musculoskeletal simulation excitation signals for the 'Default' (dashed), 'Uniform' (dash-dot-dash), and 'Custom' (solid) strength scaled models. These signals are compared to measured EMG (solid bold) and averaged between the more and less affected limbs for Participant 03. Large strength deficits measured for Participant 03's ankle plantarflexors and knee extensors resulted in predicted early onset of the gastrocnemius during stance consistent with measured EMG. RMSD from each lower-limb muscle, compared between simulated excitation signal and measured EMG is indicated for this participant for the 'Default' model (DEF), 'Uniform' model (UNIF) and 'Custom' model (CUST). Onset and duration of the excitation signal from EMG and predicted from three musculoskeletal models are shown for each muscle.

groups with substantial muscle weakness, and for individuals with substantial weakness compared to their typically developing peers. The inclusion of subject-specific or uniform strength scaling can improve gait simulations for children with CP, but it does not fully resolve the discrepancy between measured and predicted excitation patterns. The source of an individual's altered neuromuscular control strategy and resulting kinematic pattern stems from a variety of interrelated factors, including muscle weakness, altered muscle mechanics and altered neuromotor control. Therefore, assessing the influence of muscle weakness alone in this population remains challenging. For example, simulations generated for one participant in this study successfully predicted early onset of the gastrocnemius muscle and extended recruitment of the vastus lateralis throughout stance using the 'Custom' model (Fig. 4). However, agreement in this participant's tibialis anterior, medial hamstrings and rectus femoris excitations did not improve with strength scaling (Fig. 4). Although, muscle weakness is not exclusively responsible for altered gait patterns or control signals for children with CP, it appears to play a role in these altered signals.

This method of introducing subject-specific scaling was addressed within the context of assessing only EMG agreement for specific muscles in the musculoskeletal model. We acknowledge, however, there are many ways to assess the accuracy of musculoskeletal simulations. We chose this assessment as this is commonly used to validate predicted muscle activity in muscle-driven simulations (e.g., Hicks et al., 2015). In addition, accurate excitation predictions are important for many musculoskeletal simulation analyses, such as estimates of metabolic cost (e.g., Umberger et al., 2003) and muscle coordination (Knarr et al., 2014). However, EMG provides only one point of comparison with our experimental results and is often sensitive to sensor placement and contamination of excitation signals from surrounding musculature (Clancy et al., 2002). This limitation was evident in our study as the rectus femoris EMG signal from one participant and the gastrocnemius EMG signal from another participant were excluded from our analysis because of these challenges.

Estimated subject-specific strength measures revealed reduced muscle strength for our participants compared to approximated strength of their typically developing peers, consistent with previous studies (e.g. Correa and Pandy, 2011; Handsfield et al., 2014). The largest strength deficits were observed at the ankle, consistent with previous studies that quantified changes in muscle volume for

children with CP (Handsfield et al., 2016). Although we found substantial strength deficits, not all children or muscle groups had strength deficits compared to the 'Uniform' model. Specifically, the hip flexors, hip extensors, and knee flexors had greater strength compared to the 'Uniform' model. This variation in strength across lower-limb joints supports implementing custom scaling within a musculoskeletal modeling environment.

One of the advantages of the strength scaling method presented here is that, while handheld dynamometry is required, these measurements are often routinely collected as part of a child with CP's clinical examination. In contrast, full body MR imaging is rarely included as part of the diagnostic process for a child with CP. Handheld dynamometry is more affordable than comprehensive imaging of muscle volumes, yet still provides important information regarding non-uniform muscle weakness. However, imaging of muscle volumes provides greater detail and does not depend on muscle recruitment optimization criteria, and thus likely has greater accuracy in representing specific individuals when time and resources allow for these measurements. We expect that incorporating muscle volumes and muscle moment arms in a subject-specific model would result in greater differences with a uniformly-scaled model compared to our 'Custom' model. In addition, we chose to represent typically developing strength within the 'Uniform' model based on the scaling relationship presented in Handsfield et al (2014), because the results of this scaling approach estimated smaller scale factors (i.e., weaker muscles) compared to other similar scaling approaches. This conservative approach resulted in smaller differences in muscles strength between the 'Uniform' and ''Custom' models, and thus likely also resulted in smaller differences between the performance of the 'Uniform' and 'Custom' models in this study. We acknowledge there are many currently available anthropometric scaling approaches proposed to account for changes in muscle strength, and comparison with these different approaches may affect the results of this study (e.g., Correa and Pandy, 2011; Folland et al., 2008; Van der Krogt et al., 2016).

Altered neurological control, muscle physiology, and skeletal structure in children with CP also certainly influence simulation accuracy and are difficult to incorporate into musculoskeletal models. Current models for spasticity and contracture (Van der Krogt et al., 2016), modeling approaches to estimate the influence of subject-specific anatomical variations (Bosmans et al., 2015; Modenese et al., 2018; Wesseling et al., 2014), and characterizing altered neural control strategies (Steele et al., 2015) point to ongoing work to improve subject-specific musculoskeletal modeling and provide exciting avenues for advancing musculoskeletal models of children with CP. Within the current study, we did not model altered neurological control, muscle physiology or skeletal structure. However, we mitigated these limitations by carefully selecting individuals with CP who reported limited selective control deficits, limited or no skeletal abnormalities, spasticity, and contracture. Nevertheless, individuals in this study presented with mild spasticity and contracture; which likely affects the accuracy of the predicted excitations within our model. Potential limitations of the reliability of handheld dynamometry were addressed by measuring the lower-limb isometric strength for each child multiple times until they were able to produce consistent strength measurements. In addition, children selected for this study were able to selectively isolate each joint for the isometric strength tests, improving our confidence that measured strength was representative of isometric strength for each joint. Our study is limited to high-functioning children who are able to demonstrate selective motor control and walk without assistance, and the results of this study may not extend to children with more severe GMFCS levels.

Muscle weakness is an important contributing factor to altered muscle coordination in CP, as our musculoskeletal simulations were able to reproduce muscle activity patterns for children with CP without the inclusion of altered neural control or optimization criteria within our simulation framework. Addressing limitations of generic musculoskeletal models applied to children with CP has the potential to expand their clinical translation to evaluate movement strategies and treatment interventions.

## Acknowledgements

This work was partially supported by the National Science Foundation Graduate Research Fellowship (DGE-1057607).

## Conflicts of interest statement

There are no conflicts of interest associated with this work.

## References

Anderson, F.C., 1999. A Dynamic Optimization Solution For A Complete Cycle of Normal Gait. University of Texas at Austin.
Anderson, F.C., Pandy, M.G., 1999. A dynamic optimization solution for vertical jumping in three dimensions. Comput. Methods Biomech. Biomed. Engin. 2, 201–231.
Anderson, F.C., Pandy, M.G., 2001. Dynamic optimization of human walking. J. Biomech. Eng. 123, 381–390.
Bolsterlee, B., Vardy, A.N., van der Helm, F.C.T., Veeger, H.E.J., 2015. The effect of scaling physiological cross-sectional area on musculoskeletal model predictions. J. Biomech. 48, 1760–1768.
Bosmans, L., Valente, G., Wesseling, M., Van Campen, A., De Groote, F., De Schutter, J., Jonkers, I., 2015. Sensitivity of predicted muscle forces during gait to anatomical variability in musculotendon geometry. J. Biomech. 48, 2116–2123.
Clancy, E.A., Morin, E.L., Merletti, R., 2002. Sampling, noise-reduction and amplitude estimation issues in surface electromyography. J. Electromyogr. Kinesiol. 12, 1–16.
Correa, T.A., Baker, R.J., Graham, H.K., Pandy, M.G., 2011. Accuracy of generic musculoskeletal models in predicting the functional roles of muscles in human gait. J. Biomech. 44, 2096–2105.
Correa, T.A., Pandy, M.G., 2011. A mass-length scaling law for modeling muscle strength in the lower limb. J. Biomech. 44, 2782–2789.
Crompton, J., Galea, M.P., Phillips, B., 2007. Hand-held dynamometry for muscle strength measurement in children with cerebral palsy. Dev. Med. Child Neurol. 49, 106–111.
Dallmeijer, A.J., Rameckers, E.A., Houdijk, H., Groot, S., De Scholtes, V.A., Becher, J.G., 2017. Isometric muscle strength and mobility capacity in children with cerebral palsy. Disabil. Rehabil. 39, 135–142.
Delp, S.L., Anderson, F.C., Arnold, A.S., Loan, P.J., Habib, A., John, C.T., Guendelman, E., Thelen, D.G., 2007. OpenSim: open-source software to create and analyze dynamic simulations of movement. IEEE Trans. Biomed. Eng. 54, 1940–1950.
Delp, S.L., Loan, P.J., Hoy, M.G., Zajac, F.E., Topp, E.L., Rosen, J.M., 1990. An interactive graphics-based model of the lower extremity to study orthopaedic surgical procedures. IEEE Trans. Biomed. Eng. 37, 757–767.
Eek, M.N., Tranberg, R., Beckung, E., 2011. Muscle strength and kinetic gait pattern in children with bilateral spastic CP. Gait Posture 33, 333–337.
Elder, G., Kirk, J., Stewart, G., Cook, K., Weir, D., Marshal, A., Leahey, L., 2003. Contributing factors to muscle weakness in children with cerebral palsy. Dev. Med. Child Neurol. 45, 542–550.
Folland, J.P., Mc Cauley, T.M., Williams, A.G., 2008. Allometric scaling of strength measurements to body size. Eur. J. Appl. Physiol. 102, 739–745.
Fox, M.D., Reinbolt, J.A., Ounpuu, S., Delp, S.L., 2009. Mechanisms of improved knee flexion after rectus femoris transfer surgery. J. Biomech. 42, 614–619.
Friederich, J.A., Brand, R.A., 1990. Muscle fiber architecture in the human lower limb. J. Bomechanics 23, 91–95.
Handsfield, G.G., Meyer, C.H., Abel, M.F., Blemker, S.S., 2016. Heterogeneity of muscle sizes in the lower limbs of children with cerebral palsy. Muscle and Nerve 53, 933–945.
Handsfield, G.G., Meyer, C.H., Hart, J.M., Abel, M.F., Blemker, S.S., 2014. Relationships of 35 lower limb muscles to height and body mass quantified using MRI. J. Biomech. 47, 631–638.
Hegarty, A.K., Kurz, M.J., Stuberg, W., Silverman, A.K., 2016. Changes in mobility and muscle function of children with cerebral palsy after gait training: a pilot study. J. Appl. Biomech. 32, 469–486.
Hicks, J., Uchida, T.K., Seth, A., Rajagopal, A., Delp, S.L., 2015. Is my model good enough? Best practices for verification and validation of musculoskeletal models and simulations of movement. J. Biomech. Eng. 137, 1–24.
Klein Horsman, M.D., Koopman, H.F.J.M., van der Helm, F.C.T., Prosé, L.P., Veeger, H. E.J., 2007. Morphological muscle and joint parameters for musculoskeletal modelling of the lower extremity. Clin. Biomech. 22, 239–247.
Knarr, B.A., Higginson, J.S., 2015. Practical approach to subject-specific estimation of knee joint contact force. J. Biomech. 48, 2897–2902.

Knarr, B.A., Reisman, D.S., Binder-Macleod, S.A., Higginson, J.S., 2014. Changes in predicted muscle coordination with subject-specific muscle parameters for individuals after stroke. Stroke Res. Treat. 2014, 1–7.
Kurz, M.J., Corr, B., Stuberg, W., Volkman, K., Smith, N., 2011. Evaluation of lower body positive pressure supported treadmill training for children with cerebral palsy. Pediatr. Phys. Ther. 23, 232–239.
Liu, M.Q., Anderson, F.C., Pandy, M.G., Delp, S.L., 2006. Muscles that support the body also modulate forward progression during walking. J. Biomech. 39, 2623–2630.
Lu, T.-W., O'Connor, J.J., 1999. Bone position estimation from skin marker co-ordinates using global optimisation with joint constraints. J. Biomech. 32, 129–134.
Malanga, G., Mautner, K., 2017. Musculoskeletal Physical Examination, An Evidence Based Approach. Elsevier, Philadelphia.
Modenese, L., Montefiori, E., Wang, A., Wesarg, S., Viceconti, M., Mazzà, C., 2018. Investigation of the dependence of joint contact forces on musculotendon parameters using a codified workflow for image-based modelling. J. Biomech. 73, 108–118.
Mudge, A.J., Bau, K.V., Purcell, L.N., Wu, J.C., Axt, M.W., Selber, P., Burns, J., 2014. Normative reference values for lower limb joint range, bone torsion, and alignment in children aged 4–16 years. J. Pediatr. Orthop. Part B 23, 15–25.
Neptune, R.R., Kautz, S.A., Zajac, F.E., 2001. Contributions of the individual ankle plantar flexors to support, forward progression and swing initiation during walking. J. Biomech. 34, 1387–1398.
Oberhofer, K., Stott, N.S., Mithraratne, K., Anderson, I.A., 2010. Subject-specific modelling of lower limb muscles in children with cerebral palsy. Clin. Biomech. 25, 88–94.
Pandyan, A.D., Johnson, G.R., Price, C.I., Curless, R.H., Barnes, M.P., Rodgers, H., 1999. A review of the properties and limitations of the Ashworth and modified Ashworth Scales as measures of spasticity. Clin. Rehabil. 13, 373–383.
Serrancolí, G., Kinney, A.L., Fregly, B.J., Font-Llagunes, J.M., 2016. Neuromusculoskeletal model calibration significantly affects predicted knee contact forces for walking. J. Biomech. Eng. 138, 1–11.
Steele, K.M., Rozumalski, A., Schwartz, M.H., 2015. Muscle synergies and complexity of neuromuscular control during gait in cerebral palsy. Dev. Med. Child Neurol. 57, 1176–1182.
Steele, K.M., Seth, A., Hicks, J., Schwartz, M.H., Delp, S.L., 2013. Muscle contributions to vertical and fore-aft accelerations are altered in subjects with crouch gait. Gait Posture 38, 86–91.
Stuberg, W., Temme, J., Kaplan, P., Clarke, A., Fuchs, R., 1991. Measurement of tibial torsion and thigh-foot angle using goniometry and computed tomography. Clin. Orthop. Relat. Res. 272, 208–212.
Thelen, D.G., Anderson, F.C., Delp, S.L., 2003. Generating dynamic simulations of movement using computed muscle control. J. Biomech. 36, 321–328.
Umberger, B.R., Gerritsen, K.G.M., Martin, P.E., 2003. A model of human muscle energy expenditure. Comput. Methods Biomech. Biomed. Engin. 6, 99–111.
Van der Krogt, M.M., Bar-On, L., Kindt, T., Desloovere, K., Harlaar, J., 2016. Neuro-musculoskeletal simulation of instrumented contracture and spasticity assessment in children with cerebral palsy. J. Neuroeng. Rehabil. 13, 1–11.
Wesseling, M., Groote, F. De, Jonkers, I., 2014. The effect of perturbing body segment parameters on calculated joint moments and muscle forces during gait. J. Biomech. 47, 596–601.
Wickiewicz, T.L., Roy, R.R., Powell, P.L., Edgerton, V.R., 1983. Muscle architecture of the human lower limb. Clin. Orthop. Relat. Res. 179, 275–283.
Yamaguchi, G.T., Zajac, F.E., 1989. A planar model of the knee joint to characterize the knee externsor mechanism. J. Biomech. 22, 1–10.
Zajac, F.E., 1989. Muscle and tendon: properties, models, scaling, and application to biomechanics and motor control. Crit. Rev. Biomed. Eng. 17, 359–411.
Zhou, J., Butler, E.E., Rose, J., 2017. Neurologic correlates of gait abnormalities in cerebral palsy: implications for treatment. Front. Hum. Neurosci. 11, 1–20.